RSC Advances

ROYAL SOCIETY OF CHEMISTRY

www.rsc.org/advances

RSC Advances

RSCPublishing

ARTICLE

Differentially cross-linkable core-shell nanofibers for tunable delivery of anticancer drugs: Synthesis, characterization and its anticancer efficacy

Cite this: DOI: 10.1039/x0xx00000x

S. Uday Kumar[a], I. Matai[a], P. Dubey[a], B. Bhushan[a], A. Sachdev[a] and P.Gopinath[a,b]

Received xxxxxxxxxxxx
Accepted xxxxxxxxxxxx

DOI: xxxxxxxxxxxxxxxx

www.rsc.org/

This work introduces a new dimension for controlled drug delivery by nanofiber based scaffolds for anticancer therapy. The model anticancer drugs adapted in this work are curcumin and 5-fluorouracil (5-FU). Most of the drug loaded nanofibers synthesized thus far have failed to address the needs of personalized medication due to poor scalability of drug loading and delivery kinetics. This work opens up new avenues for circumventing such complications by altering the drug release profile by simple one-step crosslinking reaction. With an aim to emphasize upon the role of polymer crosslinking on drug release kinetics, two variations of dual drug loaded core-shell nanofibers were synthesized with different extent of crosslinking and polymer composition. These two variations of drug loaded nanofibers exhibited contrasting 5-FU release profile and thus manifested different therapeutic efficacy at different time points against A549 (Non-Small Cell Lung cancer) cells. The drug release profile of these fibers was further corroborated with different kinetic models to gain a perspective on the underlying mechanism driving the drug release from type I and type II nanofibers. The synergistic therapeutic potential of curcumin and 5-FU loaded core-shell nanofibers (type I and type II nanofibers) was also validated against A549 cells. As an outcome of this work, a clear correlation of cell viability with time lag in drug delivery in the case of type I and type II nanofibers could be drawn, which makes nanofiber based drug delivery even more flexible and therapeutically effective with minimal side effects.

1. Introduction

Electrospinning is a versatile and cost effective means of fabricating polymeric nanofibers. Ever since its inception it has evolved to confer diverse nanostructures and microstructures to wide range of polymers[1]. These polymeric nanofibers have already established their share of success in the field of filtration, tissue engineering, textile industry, pharmaceutics and electronics[2]. Such polymeric biodegradable scaffolds at the nanoscale act as an excellent interface to blend-in the difference between the biomaterials and biological components as they closely mimic the extracellular matrix of *in-vivo* system. Since long past such biocompatible polymeric nanofibers have witnessed extensive application in the field of tissue engineering[3]. The electrospinning technique as such enables uniform incorporation of bioactive molecules and nanoparticles in the nanofiberous polymeric matrix. Nanofibers by virtue of being at the nanoscale have large surface area to volume ratio and thus significant fraction of drugs loaded in these nanofibers are held on the nanofiber surface by weak physical forces. It is these loosely adsorbed drug molecules on the nanofiber surface that account for brief burst release of drug in the initial phase of drug release study[4]. As most of the nanofiber based anticancer drug delivery systems are associated with such burst release phase, they do not meet the basic criteria of providing a controlled and sustained drug release profile. An alternative approach to overcome such issues would be to introduce a diffusion barrier between the drugs loaded polymer phase and simulated release medium. In this case, the drug molecules would have to permeate across the passive barrier by diffusion to arrive at the release medium. This additional passive and permissive barrier regulates the drug release kinetics at an additional level. With this as the basis, in this work core–shell nanofiber with anticancer drug loaded core and a cross-linked shell barrier has been sought as a controlled and sustained drug delivery system for treatment of lung cancer.

Lung cancer is the second most prominently diagnosed cancer in the world[5]. A number of anticancer drugs have been evaluated for their efficacy against lung cancer. A major problem associated with such drugs is their therapeutic efficacy, drug resistance, specificity, bioavailability, bystander effects and the availability of suitable therapeutic formulation for appropriate means of administration. In this work, major emphases is being laid on attaining better therapeutic efficacy at lower drug dosages by using a combination of drugs with synergistic effects and at the same time improve their bioavailability by employing a nanofiber based drug delivery scaffold[6]. Such a system would aid to circumvent the problems associated with patient's predisposal to higher drug dosage levels and thereby ameliorate the health of the patient

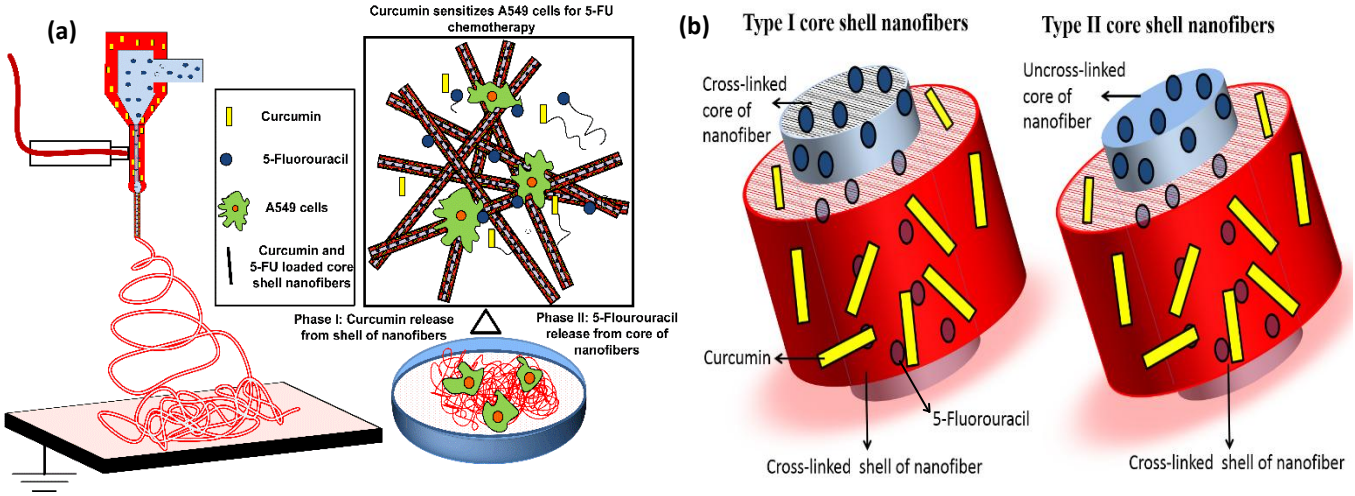

Fig. 1 Schematic outline of (a) Drug loaded PEO- PEI core-shell nanofibers fabrication by co-axial electrospinning and their antiproliferative effects against A549; (b) type I and type II nanofibers.

Pre-existing literature strongly supports the synergistic anticancer efficacy of curcumin and 5-FU, and the cellular signaling pathways by means of which they attain this synergism have also been elucidated in the past[7]. 5-FU mediates its antineoplastic effects by inhibiting the activity of thymidine synthetase (TS) enzyme which otherwise actively participates in metabolic reactions involved in nucleic acid synthesis (RNA and DNA). Owing to TS inactivation by 5-FU, the cellular nucleic acid composition is altered, which further leads to mis-incorporation of bases and the multiple lethal mutations that arise because of this, effectuates cell death. A major drawback associated with 5-FU as chemotherapeutic agent is its short life time and its catabolism in liver by an enzyme called dihydro pyrimidine dehydrogenase (DPD). As high as 80% of 5-FU administered is primarily in-effectuated by catabolic reactions in liver[8].

The plant polyphenol, curcumin being loaded in the shell of the nanofibers is released in the initial phase and sensitizes the cancer cells for 5-FU anticancer activity. In addition to this, curcumin has been found to down-regulate growth factor receptor expression in cancer stem cell which counteracts the chances of cancer recurrence after 5-FU chemotherapy [9]. With the above mentioned convictions as the basis, in this work we fabricate core-shell nanofibers loaded with 5-FU and curcumin in core and shell of the nanofibers, respectively.

Apart from this, an attempt has been made to independently fine tune the release profile of drugs loaded in core and shell of nanofibers in order to meet the needs of personalized cancer medication. This controlled and sustained drug release is attained by two critical fabrication steps, one by altering the crosslinking time and the other by altering the core polymer composition. In principle, by both means stated above, the dissolution of the polymer in hydrophilic environment is altered so as to attain a favorable drug release profile.

2. Results and discussion

2.1 Characterization of core-shell morphology of nanofibers

The FE-SEM micrographs of drug loaded type I and type II PEO-PEI nanofibers (Fig 2) revealed that both type I and type II core-shell nanofibers were of uniform diameter of 103 ±13 nm and 119 ±14.97 nm, respectively.

There were no significant difference in overall fiber morphology of type I and type II nanofibers. Owing to difference in core and shell polymer composition of type II nanofibers, core shell morphology was clearly discernable under FE-SEM as compared to that of type I nanofibers (Fig 2(c)&(d)). The surfaces of both the fibers were irregular to certain extent due to higher polymer concentration in the shell solution. The difference in PEO weight percentage in core and shell solution was adapted in order to retain the core and shell layers intact in the polymeric droplet at the needle tip and also to provide sufficient viscous drag to the core solution so as to maintain the core-shell morphology throughout the process of nanofiber extrusion, stretching and whipping. As observed in FE-SEM images of nanofibers, the core of the fibers was smooth and of uniform diameter throughout i.e. ~ 45 nm for type II and ~ 58 nm for type I.

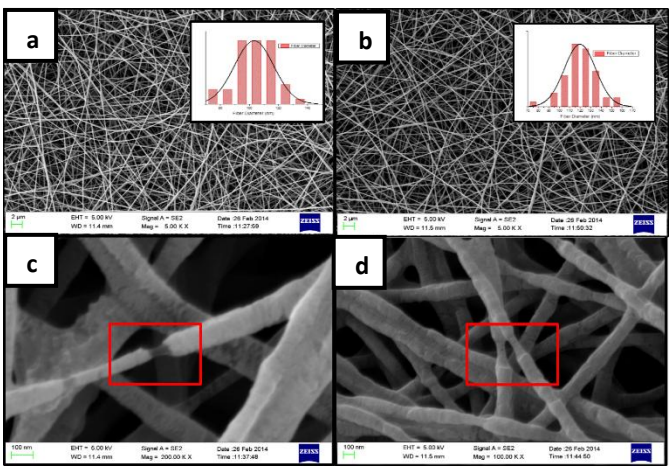

Fig. 2 FE-SEM images of Type II core-shell nanofibers (a), (c) and Type I core-shell nanofibers (b), (d) with insets showing mean fiber diameter and fiber diameter distribution.

To further confirm the core-shell structure the PEO core of type II PEO-PEI core-shell nanofibers was extracted in water and observed by TEM (Fig 3(b)). The contrast of nearly hollow core of PEO extracted nanofiber clearly established the presence of intact and distinct 5-FU loaded PEO core

throughout the core-shell nanofibers. After 24 hours incubation in release medium (PBS) a considerable increase in nanofiber diameter (i.e. from 126±9 nm to 223±12 nm) could be observed due to water permeation and retention (Fig3 (c)&(d)). The concentricity of core with respect to shell was consistent throughout the nanofiber(Fig3(d)). The contrast observed between hollow core and intact shell of nanofibers in TEM arises due to variable electron beam diffraction. Similarly, in the case of type I nanofibers, fiber diameter increased from 118±4 nm to 141±5 nm after 24 hours of incubation in PBS(Fig3 (a)&(b)).

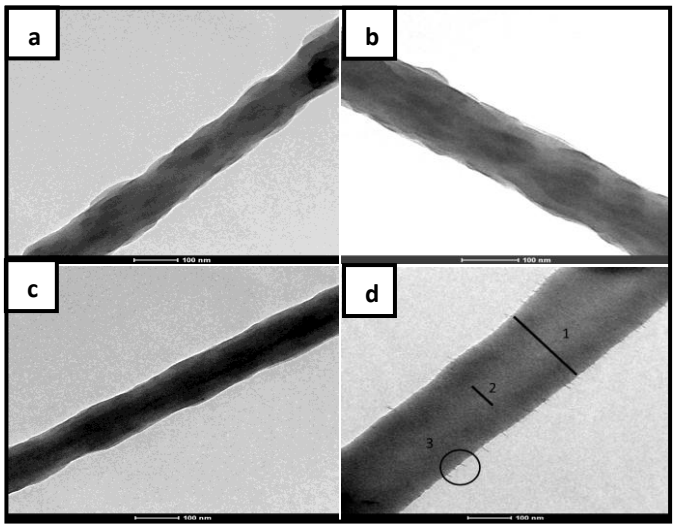

Fig. 3 TEM micrograph of type I nanofibers (a) before (b) after 24 hours incubation in PBS, type II nanofibers (c) before and (d) after 24 hours incubation in PBS

2.2 Functional characterization of core-shell nanofibers

Drug entrapment efficiency

The drug entrapment efficiency for curcumin and 5-FU in type I and type II was found to be almost equivalent as same amount of drug (i.e. 3.5 wt% of PEO) was supplemented to the polymer blend and a similar flow rate was adapted in both the cases. The entrapment efficiency of 5-FU was estimated to be 75% ±7% and 56%±4% for curcumin. The lower encapsulation efficiency is ascribed to polymer loss during electrospinning process and partly to limits of curcumin detection by UV-Vis spectrophotometer at lower concentrations.

Degree of swelling and weight Loss

As clearly evident from the TEM micrographs of nanofibers (Fig 3(c),(d)) the type II nanofibers undergoes relatively higher extent of swelling and dissolution as compared to type I nanofibers when incubated in PBS. This contrasting characteristics of type I and type II nanofibers is said to arise because of difference in core composition and extent of crosslinking. In type II nanofibers the core being PEO alone is relatively more permissive to swelling and polymer dissolution as compared to the crosslinked core of type I nanofibers. The degree of swelling and weight loss calculated for type I and type II nanofibers was also in correlation with these observations; for type I nanofibers degree of swelling was estimated to be 15% and for type II nanofibers and it was found to be 34 % at the end of 24 hours of incubation. The role of degree of swelling and weight loss (i.e. polymer dissolution) in drug release from type I and type II nanofibers has been elucidated further in drug release kinetics models described in the following discussion.

Contact angle analysis

The type I and type II nanofibers were hydrophilic nature due to inherent hydrophilic nature of base polymers i.e. PEO and bPEI. In spite of their overall hydrophilic nature a considerable difference in hydrophilicity was observed due to drug loading and crosslinking reaction (Fig 4). The bare type I and type II core-shell nanofibers exhibited hydrophilic nature with contact angle of 51.9 ±0.64 and 57.8 ±0.92 (Fig4 (a)&(b)). Inclusion of 5-FU and curcumin in core and shell of nanofibers increased the contact angle to 73.4 ±0.56 and 76.1 ±0.75. The presence of hydrophobic curcumin in the nanofiber shell layer has rendered slight hydrophobicity to nanofibers (type I and type II) and this accounts for the increase in contact angle. Whereas, in the case of their crosslinked counterparts a small decline in contact angle (i.e. 60.4 ±0.44 and 68.4 ±0.37, respectively) observed owing to gluteraldehyde content and gluteraldehyde mediated surface modification (crosslinking)[10].

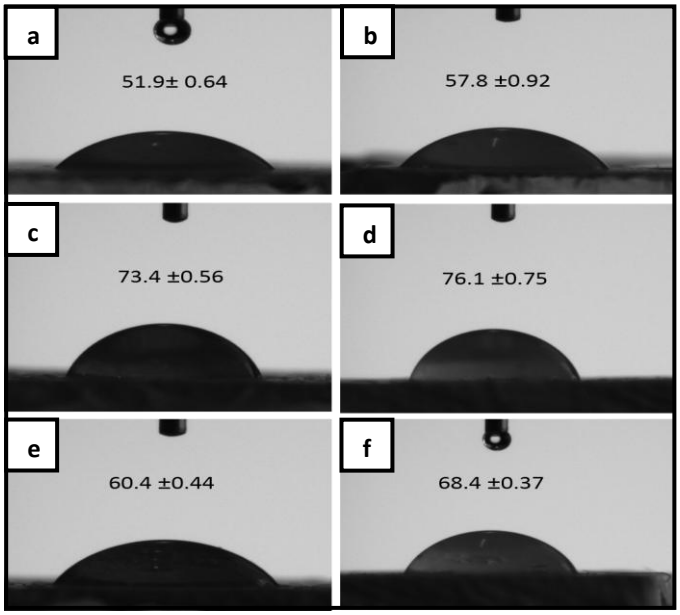

Fig. 4 Contact angle measurement for (a) type I and (b) type II bare PEO-PEI core-shell nanofibers; (c) type I and (d) type II 5-FU and curcumin loaded PEO-PEI core-shell nanofibers; (e) type I and (f) type II crosslinked 5-FU and curcumin loaded PEO-PEI core-shell nanofibers.

TG Analysis

As evident from the TG analysis of PEO-PEI nanofibers, crosslinked nanofibers have slower degradation profile indicating their improved stability as compared to that of uncrosslinked nanofibers (Fig 5). The amine group interchain covalent linkages generated during crosslinking reaction accounts for the improved thermal stability of nanofibers. The addition of drugs in the nanofibers shifts the degradation temperature by 50ºC towards the lower end[11]. This shift in degradation profile between PEO-PEI nanofibers and drug loaded nanofibers clearly suggests that curcumin and 5-FU molecules are inculcated in between polymer chains and are also involved in strong solid state interaction with the

polymeric matrix. The long chain intermolecular hydrogen boding in the polymer is interfered by the presence of drug molecules, and the presence of polymer chains around drug molecules hinders with the intermolecular hydrogen bonding in curcumin molecule. Owing to such polymer chain interferences crystalline curcumin is transformed to amorphous form. The amorphous nature of curcumin loaded in the polymeric fibers improves its dissolution in aqueous solution and thereby increases the bioavailability of curcumin. In general, both curcumin and 5-FU degrade in single step in the temperature range of 210º-400 ºC and 240º-320 ºC, respectively and this also contributes to a certain extent for the difference in degradation temperature between drug loaded and bare PEO-PEI nanofibers[12-14]. The initial mass loss up to 120 ºC is said to arise because of loss of remnant moisture and crosslinking agent in the fibers. The absence of sharp deflection in the TGA spectra indicates that the polymer and drug composition is homogenous throughout the polymer.

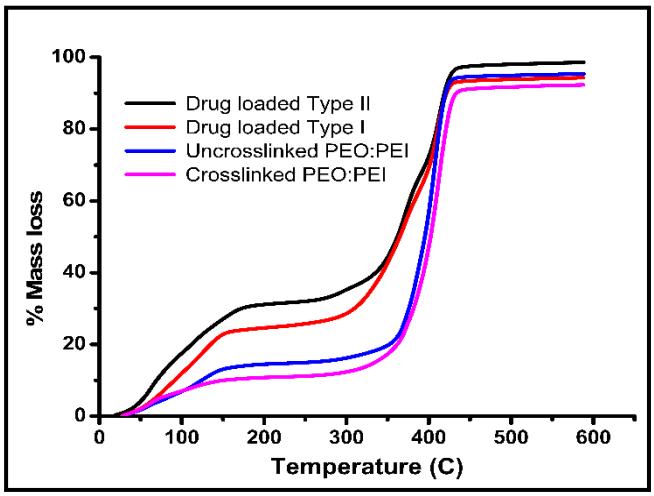

Fig. 5 TGA analysis of crosslinked and drug loaded nanofibers

XRD analysis

Bare core-shell PEO-PEI nanofibers and drug (5-FU and curcumin) loaded PEO-PEI core-shell nanofibers were analyzed by XRD to further elucidate drug physical state (intactness in therapeutically active form) and its distribution in the electrospun polymer nanofibers. The PEO-PEI nanofibers gave a characteristic semi-crystalline peak of PEO at 2θ = 23.86˚[15]. The XRD patterns of drug loaded nanofibers also depicted a broadened peak at same position (i.e. 2θ = 23.86˚) and did not possess crystalline peaks characteristic of curcumin[16] and 5-FU[17] (Fig 6). This finding confirms the absence of disordered crystalline pockets of drugs and also indicates uniform distribution of drugs throughout the polymer nanofiber. The amorphous nature of the drug in the nanofibers is further established by TG analysis and FTIR analysis.

FTIR analysis

The PEI molecules present in core-shell nanofiber is covalently crosslinked by gluteraldehyde. The two aldehyde groups at the ends of gluteraldehyde moiety generate Schiff's base by interacting with two amine groups of bPEI molecule in the proximity. The bPEI moiety has 25 % primary amine and 50% secondary amine groups, though both can react with gluteraldehyde, primary amines have higher reactivity as

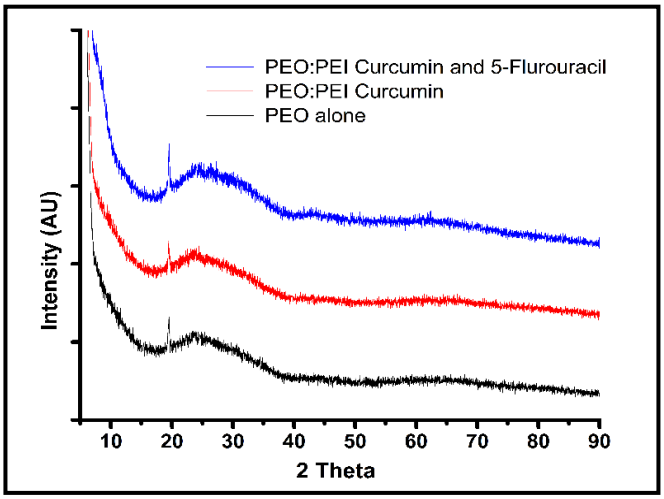

Fig. 6 XRD plot of bare PEO-PEI nanofibers and drug loaded PEO-PEI nanofibers.

compared to secondary amines[18, 19].

A strong decline in absorbance for free $-NH_2$ stretching vibration at 1640 cm^{-1} was observed for gluteraldehyde treated PEO-PEI as compared to PEO-PEI(Fig 6). This difference in spectra can be ascribed to reduction of free amine groups of PEI moiety as a certain fraction of them are involved in imide bond formation in gluteraldehyde mediated crosslinking reaction, and thus indicating the completion of reaction (Fig. S1). Further, a relative increase in stretching vibration of C=O (1566 cm^{-1}) group involved in imide bond also confirms introduction of additional imide groups during the crosslinking process. The other characteristic peaks of PEO and bPEI (at 1342 cm^{-1}, 1099 cm^{-1}, 960 cm^{-1} and 842 cm^{-1}) are retained at their respective position in the crosslinked PEO-PEI blend indicating the absence of any other polymeric interaction.

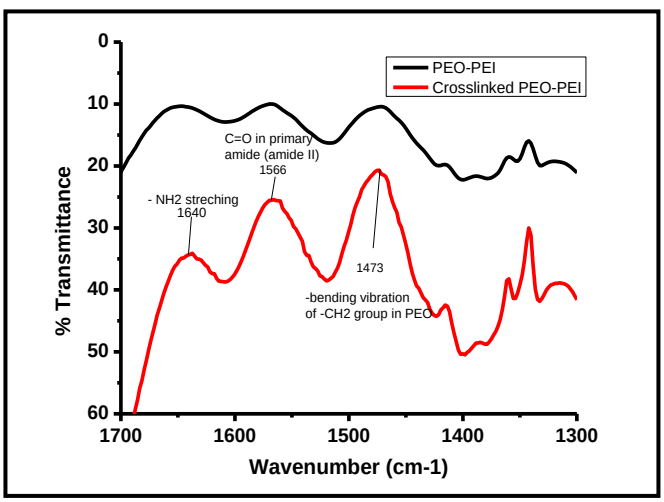

Fig. 7 FTIR spectra of PEO- bPEI and crosslinked PEO- bPEI. nanofibers.

The slight shift in characteristic curcumin bands at 1426 cm^{-1} (C-H bending vibration) and 1510 cm^{-1} (stretching vibration of C-C) in IR spectra of curcumin-PEO blend clearly indicates that PEO interferes in intermolecular hydrogen bonding of

curcumin (Fig. S2) [20]. The presence of such intermolecular hydrogen bonding facilitates in retaining curcumin in amorphous state. The amorphous curcumin has been found to have improved solubility and bio-distribution in *in-vivo* conditions as compared to its crystalline counterpart. Apart from this, FTIR study also confirms absence of covalent interaction of 5-FU and curcumin with PEO and PEI as their respective peaks are retained in IR spectra of blends at core and shell composition.

AFM analysis

The events of polymer crosslinking and polymer dissolution are surface phenomenon which leads to morphological changes in nanofibers surface and thus are investigated effectively by AFM. As both type I and type II fiber underwent polymer dissolution with respect to time of incubation in hydrophilic environment, the homogenous surface characteristics of such treated samples clearly indicates the extent and uniformity of crosslinking reaction (Fig. 9). Type I nanofiber retained their structure intact as compared to type II nanofibers after 96 hours of incubation in PBS. The selective dissolution of core in type II nanofibers was clearly evident from the parallel tracks (representing individual fibers) observed in the AFM images (Fig. 9(b)). In the case of type I nanofibers irregular depressions were observed throughout the nanofiber surface indicating slow and gradual polymer dissolution (Fig. 9(a)).

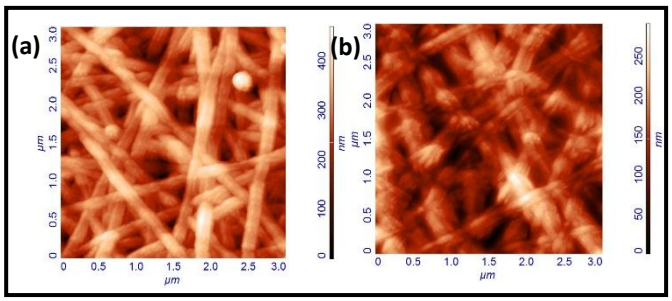

Fig 9. AFM images of (a) type I and (b) type II nanofibers after 96 hours incubation in PBS.

2.3 Drug release study

Drug release from crosslinked and un-crosslinked core shell nanofibers

To overcome initial burst release of drugs from type I and type II nanofibers the polymer were crosslinked to different extent by gluteraldehyde vapor and amount of drug released was monitored by UV-Vis spectrophotometer after 24 hours

As shown in Fig 8(a) the percentage drug (5-FU) release from type I and type II core-shell nanofiber was observed to decline gradually with increase in crosslinking time. Such variation in

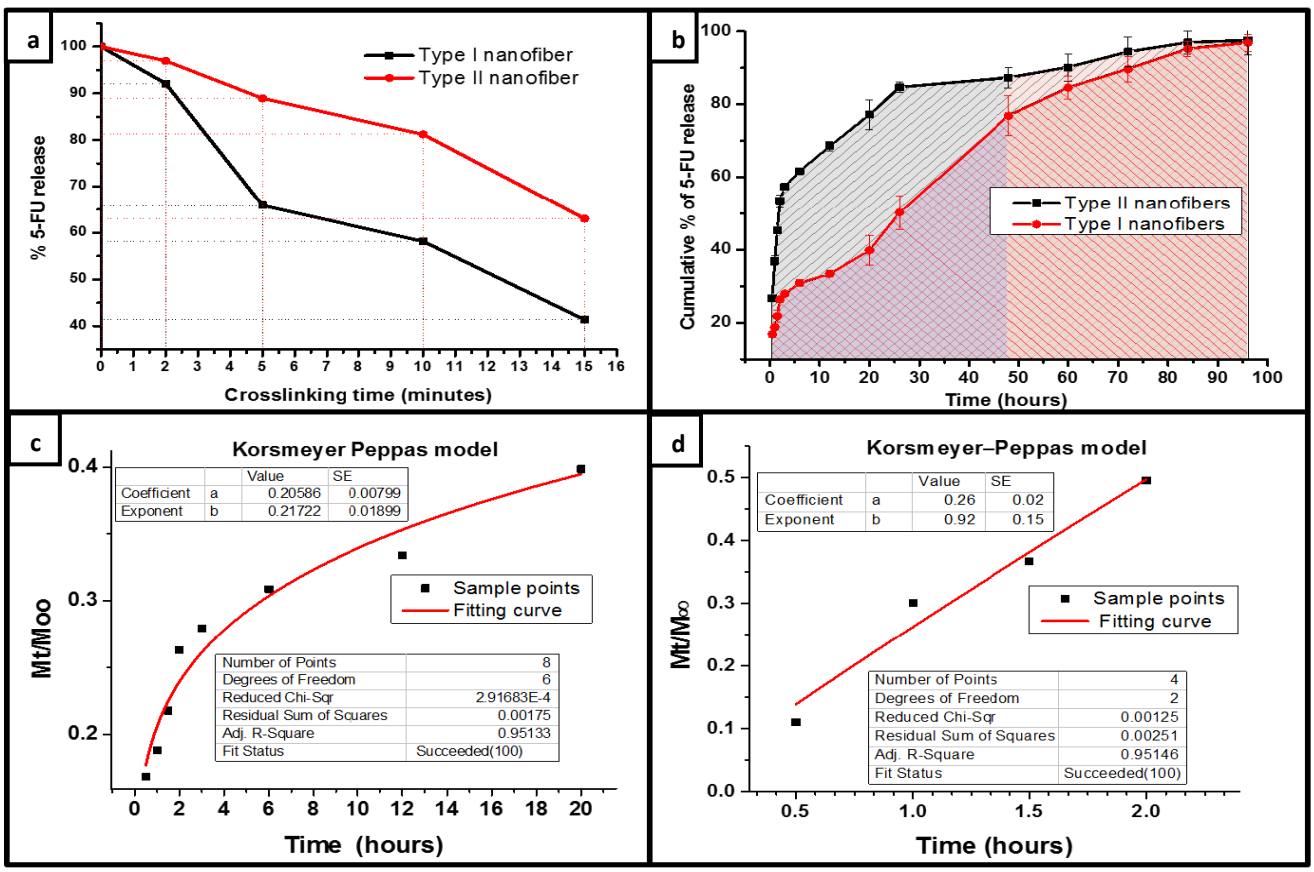

Fig. 8 (a) Effect of crosslinking on 5-FU release from type I and type II nanofibers; (b) 5-FU release profile from type I and type II core-shell nanofibers; (c) & (d) Fitting curve of Korsmeyer-Peppas model for 5-FU release profile from type I and type II nanofibers.

release profile can be attributed to slower dissolution profile of cross-linked polymers and thus slower drug diffusion. The longer fiber pretreatment with crosslinking agent (gluteraldehyde vapors) leads to higher degree of crosslinking between the amine groups of bPEI molecules in PEO-PEI nanofibers. Thus, degree of crosslinking (i.e. crosslinking time) of shell polymer (PEO-PEI) proportionately limits the extent of 5-FU permeation from core of the nanofibers. Similarly, the curcumin entrapped in the crosslinked shell of the nanofibers also diffuses out at a slower rate from crosslinked nanofibers as compared to un-crosslinked drug loaded nanofibers.

The release study establishes that there is clear correlation of the crosslinking time with the drug release profile, which extends a scope for fine-tuning the drug release profile to accomplish different therapeutic dosages in desired time spans. In both the variations of fibers (type I and type II), it was observed that 2 minutes crosslinking time did not significantly influence the release of 5-FU and curcumin from the nanofibers Fig 8(a).

At higher crosslinking time (i.e. greater than 2 minutes), a periodic shift in drug release towards the lower percentages was observed up to 15 minutes crosslinking time. Thus, the system under study has an edge over other drug delivery systems in tuning the drug diffusion rate by altering the extent of crosslinking. It is at times counter-intuitive to observe that in spite introducing crosslinks a slight initial spike in 5-FU release profile is observed. The possible explanation for this would be hydrophilic nature of core PEO polymer and small size of 5-FU which enables it to elute from the fiber with ease. The curcumin release profile from type I and type II nanofibers followed a similar trend upto 96 hours (Fig 10). Curcumin being loaded in the crosslinked nanofiber shell (in the case of type I and type II nanofibers) is released gradually without any initial burst phase. It was observed that in the case of type II nanofibers, the rate of curcumin release was marginally higher than type I. The presence of hydrophilic uncrosslinked PEO core in type II nanofibers allows greater water permeation and thus leads to slightly higher rate of curcumin dissolution from type II nanofiber than type I nanofiber.

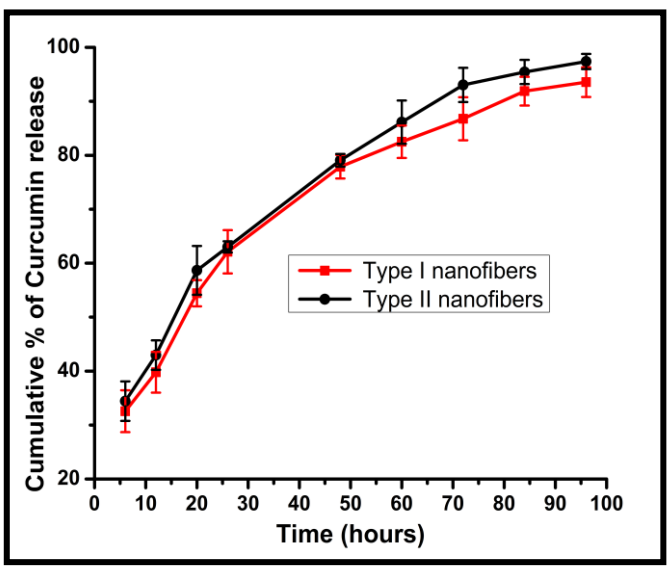

Fig 10. Curcumin release profile from type I and type II core-shell nanofibers.

Drug release kinetics for type I and type II nanofibers

The *in-vitro* release profile of drug loaded type I and type II core –shell nanofibers are shown in Fig 8(b). The 5-FU release profile from type I and type II core-shell nanofibers exhibited distinct release profile with contrasting characteristics. The initial phase of 5-FU release from type II nanofibers was relatively fast, as only the shell layer of the nanofiber was crosslinked and the highly hydrophilic PEO core containing 5-FU remained un-crosslinked. In contrary to this, both core and shell layers of type I nanofibers were cross-linked to different extent and thus resulted in controlled and sustained 5-FU release profile. In both the cases, two distinct phenomenon determine the drug release kinetics, one being the extent of solvent penetration and the other being rate of polymer dissolution. These two phenomena are said to take place at two distinct fronts i.e. diffusion front and erosion front, which migrate through the polymer matrix with passage of incubation time. In the case of type I nanofibers, the polymer composition in core and shell layer is almost same and thus all together it acts as a composite system of monolithic polymer blend with 5-FU loaded in the core. The 5-FU release profile from type I nanofibers was closely represented by Korsmeyer-Peppas model with exponent (n) value of 0.21(Fig 8(c)). The exponent value (< 0.5) clearly indicates Fickian diffusion process which arises because of swollen polymer matrix and presence of heterogeneous regions of quicker dissolution in the composite nanofiber [21]. As evident from the TEM images (Fig3 (d)) of type II nanofibers, in the initial phase of incubation, the crosslinked shell of nanofibers swells due to permeation of PBS into the nanofiber core. The core PEO containing 5-FU dissolutes the moment it comes in contact with hydrophilic environment and leaches out along with 5-FU by transcending across the crosslinked nanofiber shell.

The above mentioned mechanism clearly correlates with TEM images of the type II nanofibers (Fig3(d)) which clearly indicates swelling i.e. increase in fiber diameter (Region 1), selective dissolution of PEO core (Region 2) and the small polymer chains at boundary indicate polymer dissolution (Region 3). The presence of uniform gradient in contrast between the core and shell in nanofibers also strengthens the fact that longer PEO chains in the core diffuse toward the boundary of nanofiber shell and start accumulating at the core-shell interface.

The kinetics of 5-FU release from type II nanofibers were compared with various drug release models to consolidate upon the mechanism of drug release. The models considered under this study included zero order, first order, Higuchi and Korsmeyer-Peppas model[22]. The Korsemeyer Peppas model fitted the drug release profile to the closest extent with R^2 value of 0.95146 (Fig 8(d)). The value of exponent, n was 0.96 indicating anomalous drug transport involving both polymer swelling and Fickian diffusion. These interpretations are well in coherence with that observed in TEM images as described above.

The curcumin release kinetics in the case of type I and type II nanofibers correlated well with Korsemeyer Peppas model governing equation. The fitting curve closely represents the curcumin release profile with regression values of 0.982 and 0.987(Fig 11). The exponent values thus obtained from Korsemeyer Peppas model in both the cases (i.e 0.3678 and 0.3515) confirms Fickian diffusion as the driving mechanism for release of curcumin.

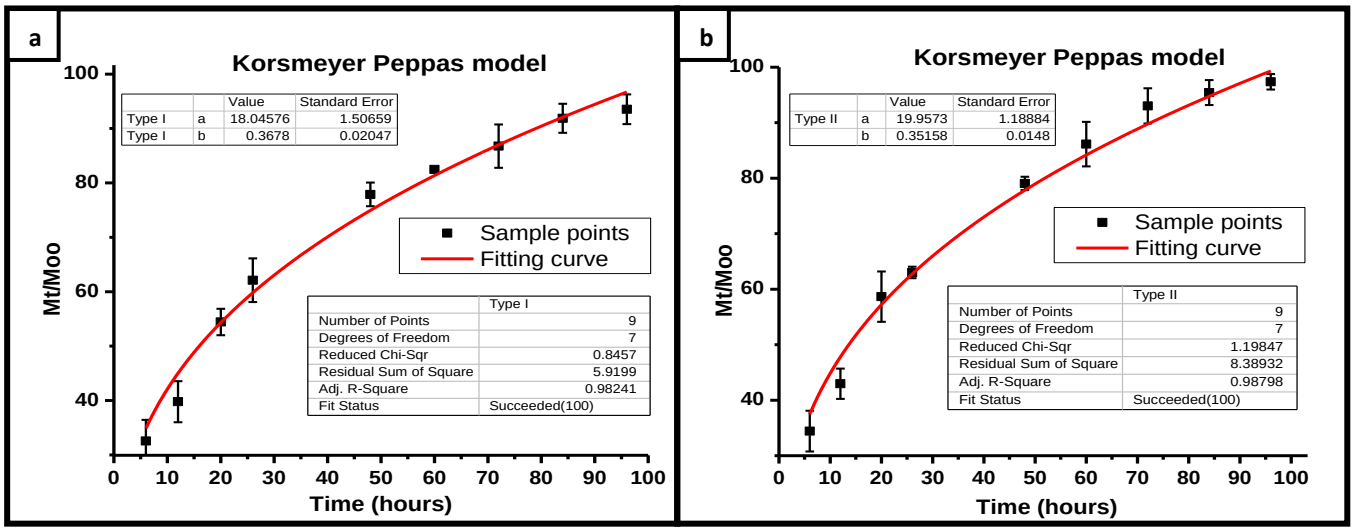

Fig 11: Korsmeyer Peppas model fitting curve for curcumin release profile from (a) type I and (b) type II core-shell nanofibers.

2.4 Cell viability assay

(a) Cell viability assay at 48 hours

The IC_{50} of curcumin and 5-FU against A549 cells was determined to be 20 µM and 3.45 µg/mL, respectively by MTT cell viability assay. The PEO-PEI nanofibers (type I and type II) biocompatibility was clearly established by A549 cell viability assay at 96 hours of seeding. In both the cases (type I and type II nanofibers) nearly equivalent (i.e. 85% and 90%) cell viability was obtained with respect to the control (Fig 12(a&b)). The anti-proliferative effect of type I and type II drug loaded core-shell nanofibers against A549 cells after 48 hours were depicted as percentage cell viability in Fig 12(a). The A549 cells seeded over core-shell nanofibers loaded with curcumin and 5-FU were found to have viability of 15% (type II) and 32% (type I). The PEO-PEI nanofibers loaded with equivalent amount of either curcumin or 5-FU alone accounted for 63% and 48% cell viability by the end of 48 hours. The sharp difference in cell viability between cells treated with either curcumin or 5-FU alone and equivalent combination of both 5-FU and curcumin clearly established their synergistic effects.

At the end of 48 hours, type I and type II nanofibers eluted around 3.14 and 3.37 µg/mL of 5-Flurouracil which was almost equivalent to IC_{50} value of 5-FU. Though type I and type II core-shell nanofibers eluted almost same amount of curcumin and 5-FU by the end of 48 hours there were huge difference in cell viability i.e. 32 % and 15% for type I and type II nanofibers, respectively. The difference in cell viability is said to arise because of difference in release profile between type I and type II core shell nanofibers (Fig8 (b)). Type I nanofibers releases majority of the drugs in the initial phase much earlier as compared to that of type II fibers. Thus, the difference in cell viability arises due to difference in duration of A549 cells exposure to effective anti-proliferative 5-FU concentration in the case of type I and type II nanofibers. To confirm the foresaid assumption A549 cells viability was estimated in a similar manner for 96 hours.

(b) Cell viability assay at 96 hours

The PEO-PEI nanofibers loaded with either curcumin or 5-FU attained cell viability of 70% and 56%, respectively. As observed in cell viability assay after 48 hours, the synergistic effects of curcumin and 5-FU were obvious in both type I and type II nanofibers by the end of 96 hours also. The percentage viability of A549 cells seeded over type I and type II nanofibers after 96 hours was found to be 21% and 23%, respectively (Fig 12(b)). These results were further correlated with study of morphology of cells seeded over type I and type II nanofibers at different time points. Such a system can be easily tuned to deliver right amount of drug in stipulated time interval, which extends a scope for attaining better therapeutic efficacy with minimum bystander effects.

Antiproliferative effects of drug loaded type I and type II nanofibers against 5-FU resistant U-87 MG cells was clearly evident at both 48 and 96 hours (Fig S4). The fibers being loaded with both curcumin and 5-FU could effectively overcome the acquired 5-FU resistance of U-87 MG cells. The difference in atiproliferative efficacy between type I and type II at 48 hours (i.e. 44%) was narrowed down to 34% at the end of 96 hours. In contrast to the case of A549 cells (where cell viability at the end of 96 hours was almost same in the case of type I and type II nanofibers at 96 hours) there was considerable difference in U-87 MG cells viability at the end of 96 hours due to 5-FU resistance. Same amount of curcumin was released at the end of 96 hours in the case of type I and type II nanofibers and considering the fact that U-87 MG is 5-FU resistant, the decline in cell viability is said to arise due to synergistic activity of 5-FU and curcumin. The curcumin release from the fiber could possibly presensitize the U-87 MG cells towards 5-FU and thus account for the above mentioned observation.

2.5 Study of cell morphology

(a) AO-EB staining

In order to discriminate between healthy cells, apoptotic cells and necrotic cells a combination of dyes, ethidium bromide

(EB) and acridine orange (AO) were used to stain the treated cells. Onset of apoptosis (programmed cell death) in cells is associated with characteristic morphological changes, which includes membrane blebbing, nuclear fragmentation and cytoplasmic constriction [23,24]. Apart from apoptosis another mechanism of cells death which is commonly observed is necrosis (cell death due to injury or trauma).

Thus, live cell's nucleus was excluded from EB stain and appeared green owing to the presence of AO alone (Fig 13(a)). AO is a cell-permeable, vital dye that intercalates into DNA and stains the cell's nucleus green (under blue filter), EB enters specifically into cells with disrupted plasma membrane and intercalates with double stranded DNA to appear orange color under green filter (Fig 13(e),(i)). Cells in early stage of apoptosis appeared bright green with spotted nucleus indicating nuclear fragmentation (Fig 13(g)). In the latter phase of apoptosis, the cell membrane undergoes blebbing and loses its intactness which leaves the cells permeable to EB. As EB stains the nucleus, cells in latter stage of apoptosis with compromised membrane integrity appear orange in color (Fig 13(d)). Apoptosis of A549 cells was observed in both the cases but at different time points, type I fibers with quicker release profile instigated apoptosis at an earlier stage as compared to type II fibers (Fig 13) The difference in number of apoptotic cells between type I and type II nanofibers were prominently observed up to 48 hours after which, apoptotic cells in both the cases (type I and type II) attained equivalent proportion (at 96 hours) which corroborates well with the equivalent amount of drug released at 96 hours from type I and type II nanofibers.

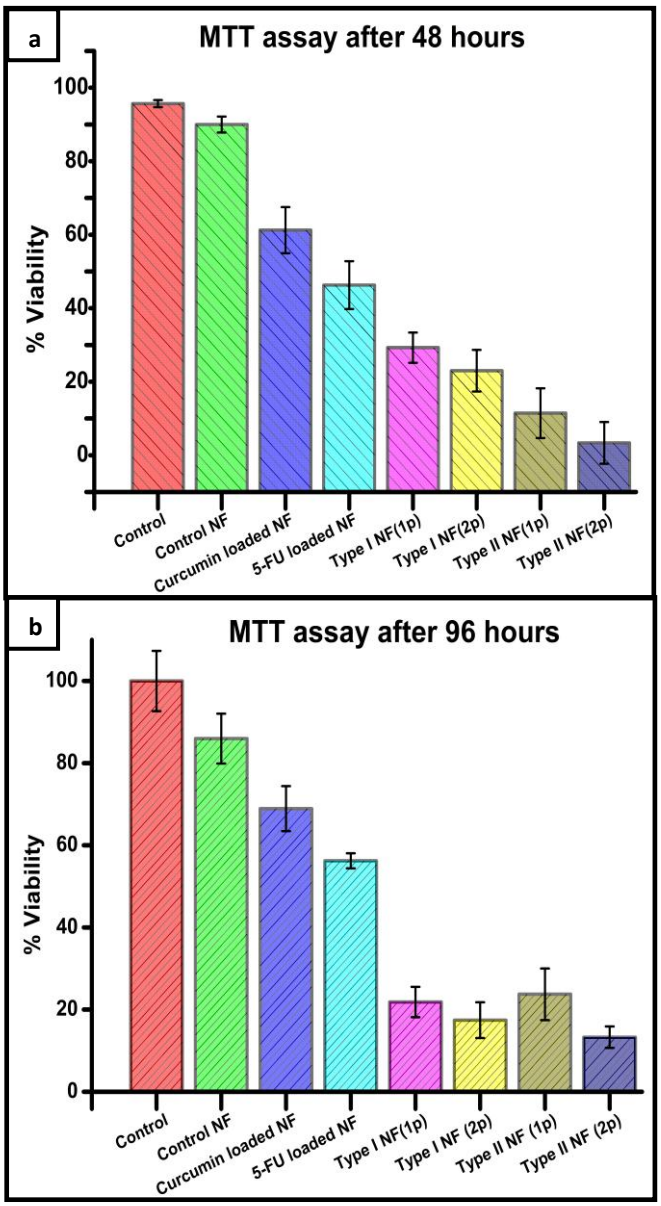

Fig 12. (a) A549 cells viability assay (MTT assay) after seeding on type I and type II nanofibers at (a) 48 hours and (b) 96 hours. *1p- Concentration of 5-FU 2.5 wt% of PEO. **2p- Concentration of 5-FU as 3.5 wt% of PEO.

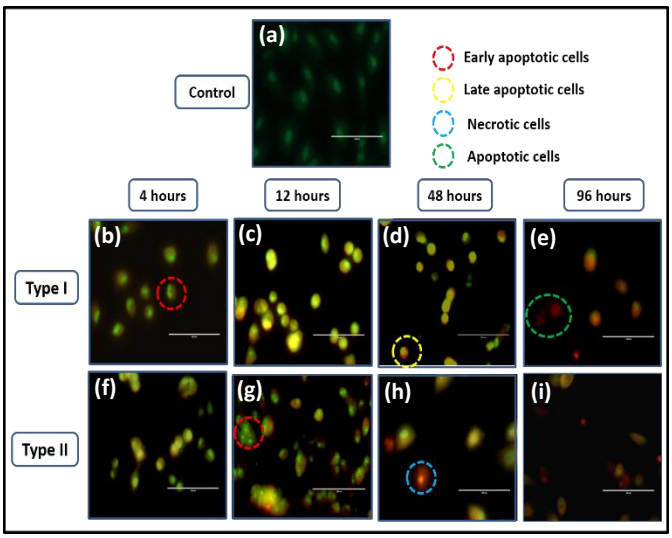

Fig 13. AO/EB stained A549 cells seeded over type I and type II nanofibers at different time points (i.e. 4 hours, 12 hours, 48 hours, 96 hours), indicating the progressive events of apoptosis.

(b) RhoB and Hoechst 33342 staining

The morphological changes in cellular components during the course of apoptosis could be easily discerned by combination of dyes RhoB and Hoechst 33342. RhoB and Hoechst 33342 stain cytoplasmic components and nucleus exclusively and thus aid in tracking subsequent cascade of apoptotic events in A549 cells seeded over drug loaded nanofibers (type I and type II) at 96 hours. The constriction of cytoplasmic volume was confirmed by drastic reduction in RhoB stained cytoplasmic components with respect to time (Fig 14(b)&(c)). Apart from this, the irregular and spotted localization of Hoechst 33342 in nucleus further confirmed the event of nuclear fragmentation in treated cells, which otherwise stains the nucleus uniformly (Fig 14(e)&(f))[25].

In certain apoptotic cells, cytoplasmic stain Rho B stained the nucleus, which clearly establishes nuclear membrane disruption (Fig 14(b)&(c)) and apoptosis**.** The auto-fluorescent nanofiberous PEO-PEI mats underneath the cells were visualized under blue filter to confirm their structural integrity during the course of therapeutic study. There was no significant morphological variation due to slower dissolution of cross-linked PEO-PEI shell of nanofibers.

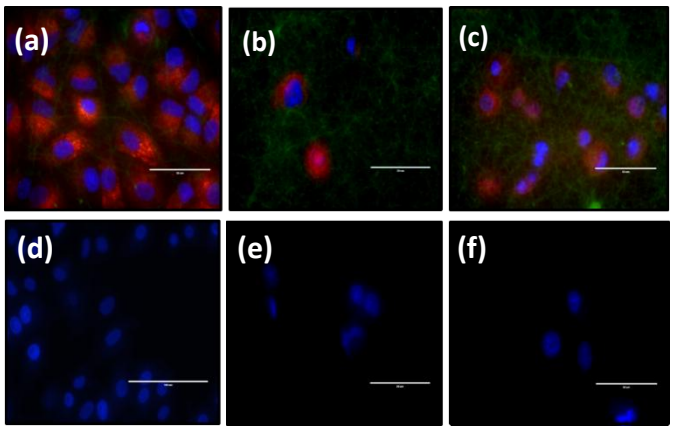

Fig 14. Rhodamine B and Hoechst 33342 stained A549 cells seeded over (a)control PEO-PEI nanofibers; (b) type I nanofibers and (c) type II nanofibers; Hoechst 33342 stained nuclei of A549 cells seeded over (d)control PEO-PEI nanofibers (e) type I nanofibers and (f) type II nanofibers.

(b) FE-SEM analysis

The FE-SEM images of A549 cells seeded over control PEO-PEI nanofibers clearly indicated that cells retain their characteristic morphology and their interaction with the polymeric fibers favored cell attachment. The close interface between the cells and polymeric fibers also improves delivery of 5-FU and curcumin loaded in type I and type II nanofibers. The A549 cells seeded over type I and type II nanofibers underwent a cascade of morphological changes characteristic of apoptosis during the 96 hours incubation period. The Fig 15(b)&(c) are representative images of A549 cells morphology after 96 hours incubation on type I and type II drug loaded nanofibers. In both the cases, the events of cytoplasmic constriction, membrane blebbing and cell lysis were prominently observed, whereas the control fibers (Fig 15(a)) were permissive to A549 cells growth and proliferation and also retained their characteristic cellular morphology at 96 hours of incubation[24].

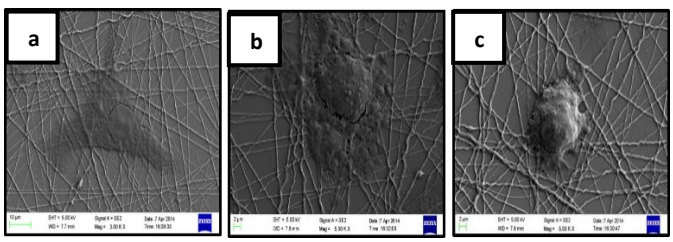

Fig 15. FE-SEM images of A549 cells seeded over (a) control nanofibers, (b) type I and (b) type II nanofibers at 96 hours

Conclusion

This work provides a scope for realizing a drug dose tunable nanofiber based drug delivery system by one-step crosslinking reaction. This additional flexibility of the PEO-PEI based nanofiber in terms of scalable release profile enables it to suffice the prerequisites for realizing personalized therapeutics. The therapeutic efficacy of two such systems i.e. type I and type II core-shell PEO-PEI nanofibers loaded with curcumin and 5-FU was evaluated at two different time points to establish the claim. The results indicated that though both the fibers were loaded with equivalent amount of drugs the cell viability at 48 hours was different in both the cases owing to the lag in drug release profile of type I nanofibers. This viability differences were nullified at 96 hours as >90% of the drugs loaded in both type I and type II nanofibers were released prior to that time point. This work also correlates the extent of polymer crosslinking to the drug release kinetics. In addition to altering the crosslinking agent concentration, in this work precursor polymer concentration is also utilised as an additional factor in controlling the extent of crosslinking. Thus, this versatile PEO-PEI based nanofiberous system can be scaled accordingly to deliver right amount of drug to the right place and at right point of time (i.e. a characteristic controlled drug delivery system). The core-shell PEO-PEI nanofibers loaded with two different drugs (5-FU and curcumin) having synergistic antineoplastic effects can overcome multiple drug resistance and reduce the chances of cancer recurrence.

This work was supported by the Science and Engineering Research Board (No.SR/FT/LS-57/2012) and Department of Biotechnology (No.BT/PR6804/GBD/27/486/2012), Government of India. Sincere thanks to Department of Chemistry and Institute Instrumentation Centre, IIT Roorkee for the various analytical facilities provided.

Notes and references

[a]*Nanobiotechnology Laboratory, Centre for Nanotechnology,*
[b]*Department of Biotechnology,*
Indian Institute of Technology Roorkee, Roorkee, Uttarakhand-247667, India. Fax: +91-1332-273560; Tel: 91-1332-285650; E-mail: pgopifnt@iitr.ernet.in, genegopi@gmail.com

† Electronic Supplementary Information (ESI) available: [details of any supplementary information available should be included here]. See DOI: 10.1039/b000000x/

References

[1] S. Koombhongse, W. Liu, D.H. Reneker, Journal of Polymer Science: Part B: Polymer Physics, 39 (2001) , 2598–2606.
[2] W.Z.M. Huang, Y.Z. Zhang, M. Kotaki, S. Ramakrishna, Composites Science and Technology, 63 (2003) 2223-2253.
[3] R. Vasita, D. S. Katti, International Journal of Nanomedicine,1(1) (2006) 15–30.
[4] D.-G. Yu, Health, 01 (2009) 67-75.
[5] U.K. Sukumar, B. Bhushan, P. Dubey, I. Matai, A. Sachdev and P. Gopinath International Nano Letters, 3 (2013) 45-53
[6] P. Gopinath, S.S. Ghosh, Molecular Biotechnology, 39 (2008) 39-48.
[7] B.B. Patel, A.P. Majumdar, Nutrition and Cancer, 61 (2009) 842-846.
[8] M. Shakibaei, C. Buhrmann, P. Kraehe, P. Shayan, C. Lueders, A. Goel, PloS one, 9 (2014) 85397-85403.
[9] F. Tian, T. Fan, Y. Zhang, Y. Jiang, X. Zhang, Acta biochimica et biophysica Sinica, 44 (2012) 847-855.
[10] M. Sampath, R. Lakra, P. Korrapati, B. Sengottuvelan, Colloids and surfaces. B, Biointerfaces, 117 (2014) 128-134.
[11] A. Mathew, T. Fukuda, Y. Nagaoka, T. Hasumura, H. Morimoto, Y. Yoshida, T. Maekawa, K. Venugopal, D.S. Kumar, PloS one, 7 (2012) 32616-32622.
[12] E. Thangaraju, N.T. Srinivasan, R. Kumar, P.K. Sehgal, S. Rajiv, Fibers and Polymers, 13 (2012) 823-830.

[13] T. Elakkiya, G. Malarvizhi, S. Rajiv, T.S. Natarajan, Polymer International, 63 (2014) 100-105.
[14] Q. Liu, Y. Bei, G. Qi, and Y. Ding, Korean Journal of Chemical Engineering, 25(5) (2008), 980-981.
[15] T. Uyar, F. Besenbacher, European Polymer Journal, 45 (2009) 1032-1037.
[16] G. Guo, S. Fu, L. Zhou, H. Liang, M. Fan, F. Luo, Z. Qian, Y. Wei, Nanoscale, 3 (2011) 3825-3832.
[17] K.K. Gupta, N. Pal, P.K. Mishra, P. Srivastava, S. Mohanty, P. Maiti, Journal of biomedical materials research. Part A, (2013) 54-67.
[18] A. Jayakrishnan, S.R. Jameela, Biomaterials, 17 (1996) 471-484.
[19] S. Deng, Y.P. Ting, Water research, 39 (2005) 2167-2177.
[20] T.M. Kolev, E.A. Velcheva, B.A. Stamboliyska, M. Spiteller, International Journal of Quantum Chemistry, 102 (2005) 1069-1079.
[21] X. Li, M.A. Kanjwal, L. Lin, I.S. Chronakis, Colloids and Surfaces. B, Biointerfaces, 103 (2013) 182-188.
[22] P. L. Ritger and N. A. Peppas, Journal of Controlled Release, 5 (1987) 37-42.
[23] P. Gopinath, S.S. Ghosh, Molecular and Cellular Biochemistry,324 (2009) 21-29.
[24] P. Gopinath, S.K. Gogoi, A. Chattopadhyay, S.S. Ghosh, Nanotechnology, 19 (2008) 75104-75109.
[25] R. Yao, A. Sui, Z. Wang, S. Liu, Q. Zhou, X. Liu, H. Zhang, Molecular Medicine Reports, 6 (2012) 1355-1360.

Graphical abstract